Cardioprotective effect of NRG-4 gene expression on spontaneous hypertension rats and its mechanism through mediating the activation of ErbB signaling pathway

Zhang Yang, Wang Yaling, Liu Tao, Rao Mingyue, Li Yongjun*

Department of Cardiology, East Hospital, the Second Hospital of Hebei Medical University, Shijiazhuang 050000, Hebei Province, P.R. China

ARTICLE INFO

ABSTRACT

To explore the myocardial protective effect of Neuregulin-4 (NRG-4) gene expression on spontaneous hypertension (SHR) rats and its mechanism through mediating the activation of the ErbB signaling pathway, this study was conducted. For this purpose, forty 24-week-old male SPF SHR rats were selected as the experimental group, and 10 age and sex-matched Wistar Kyoto (WKY) rats were selected as the control group. Cardiac tissues were collected for hematoxylin-eosin (HE) staining, terminal deoxynucleotidyl transferase-mediated dUTP-biotin nick end labeling (TUNEL) staining, Masson staining, and immunohistochemical staining. Following tail vein injection of recombinant lentiviral vectors, the experimental groups were constructed as the control group (SHR rats without any treatment), Empty vector group (Empty Vector transfection), shRNA negative control (NC) group (LV-shRNA-NRG-4 NC transfection to silence the expression of NRG-4), shRNA group (LV-shRNA-NRG-4 transfection), pcDNA3.1(-) NC group (pcDNA3.1(-)-NRG-4 empty vector transfection) and pcDNA3.1(-) group (pcDNA3.1(-)-NRG-4 transfection to overexpress NRG-4). Quantitative real-time polymerase chain reaction (qRT-PCR) and Western blot were used to detect the expression levels In addition, methyl thiazolyl tetrazolium salt (MTT) assay and flow cytometry were performed to detect the proliferation and apoptosis of cardiomyocytes, respectively. Results showed that in the SHR group, the cardiomyocytes showed hypertrophy, disordered arrangement, hyperchromatic nucleus, irregular shape, obvious rupture of myocardial fibers, and obvious proliferation of fibrous stroma; obvious myocardial fibrosis, and there were more blue collagen fibers around cardiomyocytes and myocardial arterioles; cardiomyocytes were swollen, muscle fibers arranged disorderly, collagen around the coronary artery and myocardial interstitium increased significantly with a cross-linking appearance; besides, compared with WKY group, the apoptosis index of cardiomyocytes in SHR group was significantly increased ($P<0.05$). The expression of NRG-4 protein was decreased in the SHR group compared with the WKY group ($P<0.05$). In vitro, there was no difference in the mRNA expression of NRG-4, ErbB2 and ErbB4, MMP2, TGFβ1 and α-SMA, as well as Caspase3, Bax and Bcl-2 among the control group, Empty vector group, shRNA NC group and pcDNA3.1(-) NC group ($P>0.05$). While shRNA group showed decreased expressions of NRG-4, ErbB2, ErbB4, MMP2, TGFβ1, α-SMA and Bcl-2, while increased Caspase3 and Bax expressions, as well as promoted cell proliferation and cell apoptosis when compared with the shRNA NC group ($P<0.05$); while compared with pcDNA3.1(-) NC group, pcDNA3.1(-) group had highly increased expressions of NRG-4, ErbB2, ErbB4, MMP2, TGFβ1, α-SMA and Bcl-2, while decreased Caspase3 and Bax expressions, inhibited cell proliferation and cell apoptosis (all $P<0.05$). It is concluded Upregulation of NRG-4 gene expression can promote the activation of the ErbB signaling pathway, thus inhibiting the proliferation and apoptosis of cardiomyocytes in SHR rats, reversing myocardial fibrosis, and playing its cardioprotective role.

Introduction

Cardiovascular disease has long been the leading cause of death in developed countries and is rapidly becoming the biggest killer in developing countries (1,2). In many cardiovascular diseases, hypertension, ischemic heart disease, vascular disease, and endocrine disorders, for example, cardiomyocytes may respond to hypertrophic growth due to external stimuli (3). It may be further characterized by cell enlargement, enhanced protein synthesis and myofibrillar protein aggregation, which leads to myocardial remodeling and often ends in heart failure and sudden death (4,5).

Hypertension is a major risk factor for heart disease, especially leading to the development of ischemic heart disease and eventually heart failure (6). The pathogenesis of hypertension is quite complex, which is related to many factors, such as

*Corresponding author. E-mail: lyjbs2009@yeah.net

heredity, environment, diet, stress, obesity, etc. (7,8). Existing studies have shown that sympathetic hyperactivity, renin-angiotensin-aldosterone system activation, water and sodium retention, membrane ion transport abnormalities, insulin resistance, endothelial dysfunction and others are involved in the occurrence and development of hypertension (9,10). These mechanisms interact with each other, which can lead to the thickening of the vascular wall, the decrease of elasticity, the dysfunction of relaxation and contraction, the increase of peripheral vascular resistance, resulting in the increase of blood pressure and the damage of target organs (11,12). As one of the important target organs of direct injury in hypertension, the heart may suffer from the most significant characteristic pathological change, namely, myocardial fibrosis (13). In the ventricular remodeling of hypertension, the main changes of myocardial tissue structure are cardiomyocyte hypertrophy, coronary artery changes, myocardial interstitial fibrosis and imbalance of cardiomyocyte proliferation and apoptosis (14,15). The fibrotic disease is a kind of histological change after injury or stimulation, which is characterized by excessive deposition of extracellular matrix (16). Myocardial fibrosis is a common pathological change in most cardiovascular diseases (17,18). The pathological characteristics of its formation are the aggregation, activation and proliferation of fibroblasts, the excessive deposition of extracellular matrix proteins and the excessive accumulation of collagen fibers, which may lead to cardiac tissue sclerosis, abnormal cardiac tissue structure and function (19).

Neuregulin (NRG) is a signal protein expressed in the nervous system, myocardium and other tissues (20). As a ligand, it can bind to the ErbB receptor on the cell surface, cause its conformation change to form dimer, and then activate the intracellular leucine kinase and a series of downstream signaling pathways, such as P13K/Akt, Ras/Erk, etc. (21,22). NRG gene is a member of the epidermal growth factor (EGF) gene family (23). At present, four genes with similar structures have been found, which encode NRG-1, NRG-2, NRG-3, and NRG-4 respectively (24). NRG binds to ErbB (a gene derived from the name of a viral oncogene to which these receptors are homologous: erythroblastic leukemia viral oncogene) family of tyrosine kinase

receptors (erbB2, ErbB3 and ErbB4) and plays its role through the paracrine pathway (25). ErbB receptor consists of extracellular ligand-binding domain, the transmembrane domain and intracellular tyrosine kinase domain (25). NRG binds to the ErbB4 receptor and induces its conformational change; the allosteric ErbB4 receptor changes to the activated form by binding to ErbB2 to dimer or intracellular ligand (26). Tyrosine kinase domain located in the cell can then phosphorylate the C-terminal of the other half of the dimer. The proposed process can provide binding targets for a variety of intracellular adaptor proteins, such as PI3K, thus activating downstream signaling pathways and participating in cell proliferation, differentiation and migration (27). In recent years, a large number of literatures have reported that the activation of NRG1/ErbB4 and its downstream signaling pathway is involved in the ischemic injury of a variety of tissues (mainly brain and myocardium), and this signaling pathway is considered to be involved in the inhibition of apoptosis after myocardial and cerebral ischemic injury (28,29). However, there is a rare opinion concerning the exploration of NRG4/ErbB4 in disease progression.

Spontaneous disease model refers to the establishment of a stable and uniform animal model of a combination of disease and syndrome by analyzing the characteristics of the spontaneous disease animal model. As for hypertension we concerned, our study established spontaneous hypertension (SHR) model to explore the myocardial protective effect of Neuregulin-4 (NRG-4) gene expression on SHR rats and its mechanism through mediating the activation of the ErbB signaling pathway.

Materials and methods
Preparation of experimental model

Forty 24-week-old male SPF SHR rats were selected as the experimental group, and 10 age and sex-matched Wistar Kyoto (WKY) rats were selected as the control group. All animals were purchased from the Animal Department of China Medical University, fed with standard rat feed at room temperature and raised in an environment with a relative humidity of 70%. Automatic lighting was provided from 8 am to 8 pm. Animals were provided

with free access to diets and drinks. The use of all experimental animals was approved by the local animal management agency, which was in line with the relevant management regulations. All rats were treated humanely throughout the experimental process. All rats were reared adaptively for one week. After that, the rats in the experimental group were fed with 0.45% sodium chloride solution for three weeks, and the rats in the control group drank tap water normally.

Collection of cardiac tissues for staining

Rats with SHR (n=10) and WKY rats (n=10) were anesthetized by intraperitoneal injection of 10% chloral hydrate. After that, the heart was taken out quickly. The blood was rinsed with ice PBS solution. The large blood vessels, atrium and right ventricle were cut off. The tissue was dried with sterile filter paper. The heart was cut in half along the long axis of the left ventricle. One part was fixed with 4% paraformaldehyde for morphological examination, and the other part was put into a cryopreservation tube for cryopreservation at - 80℃ in liquid nitrogen.

Hematoxylin-eosin (HE) staining

In the process of HE staining, the tissue fixed in formaldehyde was dehydrated by using ethanol solution from low to high concentration, then in the transparent agent xylene I solution and xylene II solution for 30 min each, and in the dissolved paraffin I, paraffin II and paraffin III for 40 min each. After the paraffin was completely immersed in the tissue block, the sample tissue was put into the embedding machine with pre-melted wax for paraffin embedding, and then cooled and solidified into blocks, which were preserved at room temperature. The paraffin tissue was sliced continuously with a slicer at the thickness of 4μL for storage at 37℃ overnight; the slides were baked in an oven at 70℃, and then were put into xylene I and II solution for 10 min for dewaxing. Afterward, the slides were put into different concentrations of alcohol solution from low to high for 5 min each, dehydrated, and then put into distilled water. The slides were stained in hematoxylin aqueous solution for several minutes and immediately washed with running water for a while. In the next step, the slides were put into a hydrochloric acid solution and

aluminum carbonate solution for several seconds respectively; washed under running water for 20 min and then put into distilled water; stained in eosin solution for 3 min; successively put into different concentrations of (50%, 70%, 80%) ethanol solution for 5 min respectively for dehydration. Subsequently, the slides were put into xylene again to make the slices transparent, followed by sealing with gum. The tissue sections were observed under a microscope.

Terminal deoxynucleotidyl transferase-mediated dUTP-biotin nick end labeling (TUNEL) assay

Tissues were treated with xylene twice for 5 min each time, ethanol gradient (100, 95, 90, 80, 70%) once for 3 min each, proteinase K solution for 15-30 min and PBS for 2 times. The treatment group was mixed with 550μL TdT+450μL fluorescein-labeled dUTP solution; and the negative control group was only added with 50μL fluorescein-labeled dUTP solution. The reaction was carried out in a dark wet box at 37 ℃ for 1 h. After three times of PBS washing, 50~100μLDAB substrate was added to the tissue and reacted at 15 ~ 25℃ for 10 min, followed by another three times of PBS washing and re-staining with hematoxylin. The next steps were gradient ethanol dehydration, xylene transparent processing, and neutral gum sealing. Apoptotic cells were observed by a light microscope and photographed. Under 400 times microscope, the apoptotic cardiomyocytes and the total number of cardiomyocytes were counted in 5 different fields of each section. Apoptosis index was used to reflect the apoptosis of cardiomyocytes in each group according to the formula of (number of apoptotic cells in visual field/number of all cardiomyocytes in the visual field) × 100%.

Masson staining

After routine dewaxing, hematoxylin staining was performed, the slides were stained in hematoxylin solution for 10 min and immediately washed with tap water 4-5 times. The slides were put into 1% hydrochloric acid alcohol solution for 3 s and immediately washed with tap water 4-5 times. After that, the slides were placed into Ponceau acid fuchsin for 5 min and then washed with water. Following treatment with 1% phosphomolybdic acid for 5min,

the slides were re-stained with 2% aniline blue for 5 min. After that, the slides were immersed in 1% glacial acetic acid for 1 min, quickly dripped with 95% alcohol 3 times, dehydrated, transparently processed and sealed with neutral gum. The staining of tissues was observed under a microscope. The collagen fibers were blue and the cardiomyocytes were red. The percentage of myocardial collagen fiber area in the whole tissue area was calculated by image analysis and processing system, namely, Collagen Volume Fraction (CVF)=collagen area/total area. Three visual fields were randomly selected from each specimen and the mean value was calculated.

Immunohistochemical staining

Following dewaxing and hydration described before, the tissue slices were immersed in the citric acid buffer which was heated and boiled by microwave. The tissue sections were naturally cooled at room temperature for 1 h and then cooled to room temperature. 3%H2O2 was then used to block endogenous peroxidase at room temperature for 20min, followed by 3 times of washing with PBS. The next step was sealing with goat serum at room temperature for 15-30min. After that, the primary antibody was added and then the incubation was performed in the wet box at 4℃ overnight. The next day, the tissue sections were taken out and rewarming at room temperature for about 1 h. The sections were rinsed with PBS for 5 min × 3 times. Subsequently, the secondary antibody was added for 60min of incubation at room temperature. After three times PBS washing, DAB development was performed, and the degree of staining was controlled under the microscope. Afterward, the tissue sections were rinsed with running water for 10min and re-stained with hematoxylin for 2min, followed by differentiation with hydrochloric alcohol, and the final steps were dehydration, transparent processing, sealing, and observation under the microscope. Immunohistochemical staining was scored by the German semi-quantitative system, and the positive staining intensity and area were observed under an optical microscope (100× and 400×).

Tail vein injection of recombinant lentiviral vectors

The remaining 30 SHR rats were used for further experiments according to different treatment protocols, with 5 rats in each group. According to different recombinant lentiviral vectors (GeneChem, Shanghai, China), the experimental groups were constructed as follows: blank control group (Control group; SHR rats without any treatment, as the blank control and to verify the avirulence of lentiviral vector), Empty Vector transfection group (Empty Vector group), LV-shRNA-NRG-4 NC transfection group (shRNA NC group; NRG-4 silencing empty vector control group), LV-shRNA-NRG-4 transfection group (shRNA group; NRG-4 silencing group), pcDNA3.1(-)-NRG-4 empty vector transfection group (pcDNA3.1(-) NC group; NRG-4 overexpression empty vector control group) and pcDNA3.1(-)-NRG-4 transfection group (pcDNA3.1(-) group; NRG-4 overexpression group).

Cardiomyocytes culture

Rats were operated on under aseptic conditions the following sacrifice by cervical dislocation. The heart was taken out by thoracotomy. The atrium and large blood vessels were separated and removed. The ventricle was cut into a tissue block of $1mm^3$ in volume. Following washing twice with DMEM, 0.125% trypsin was added for digestion in a water bath at 37℃ for 5 min. The trypsin was sucked and discarded, and the DMEM medium containing 15% fetal calf serum (FCS) was added for full blowing. After slightly standing, the upper cell suspension was sucked and transferred into a $25cm^2$ culture flask. Following incubation in a 5%CO2 incubator at 37℃ for 90 min, the DMEM medium containing 15% FCS was added to culture until sub-fusion state after the removal of the original culture medium. The cells were digested with 0.25% trypsin containing EDTA and subcultured, followed by further culture in a 5% CO2 incubator at 37℃.

Quantitative real-time polymerase chain reaction (qRT-PCR) for detecting NRG-4; ErbB2, ErbB4; matrix metalloproteinase 2 (MMP2), tumor growth factor β (TGFβ1) and α-smooth muscle actin (α-SMA); Caspase3, Bcl-2 associated X (Bax) and B-cell lymphoma-2 (Bcl-2) mRNA expressions

Total RNA was extracted from animal tissues according to Trizol reagent instructions. The specific steps are as follows: about 50mg of rat tissue was collected from each group and placed into a homogenizer, followed by the addition of Trizol to 1.0ml/50mg of tissue for homogenization. The homogenized sample was transferred to a 1.5ml RNase-free EP tube, and the supernatant was collected after standing at room temperature for 5min, centrifugation at 4℃ and 12,000r/min for 10min, with the supernatant collected. An amount of 0.2ml chloroform was added to every 1ml Trizol, followed by vortex oscillation for 15s, and reaction at room temperature for 3-5min. After another centrifugation at 4℃ and 12,000r/min for 15min, the supernatant was transferred to another clean centrifuge tube, then centrifuged with isopropanol, the supernatant was removed, RNA precipitate was washed with 75% ethanol, and the supernatant was discarded after centrifugation. The A260, A280 and A260/A280 values were determined by UV spectrophotometer. The purity and concentration of RNA were analyzed. The RNA was stored at - 80℃ for future use. In order to avoid the degradation of RNA, the extracted RNA should be reverse transcribed immediately. Secondly, to avoid RNase contamination of RNA samples, all laboratory supplies should be treated with DEPC, and all reaction solutions should be prepared on ice. After cDNA synthesis, RT-PCR was used to detect the mRNA expression of related genes. Specifically, the reagents needed for qPCR reaction were dissolved, turned upside down slightly, mixed well, centrifuged for a short time, and placed on ice for use. The following reagents were added to the total volume of 20ul, including 2u1 cDNA, 10ul 2xAll-in-one qPCR Mix, 2ul PCR forward/reverse primer(2uM), 0.4ul 50x Rox Reference Dye, and 3.6ul ddH2O. The qPCR reaction solution was mixed well, added to the PCR reaction tube, and centrifuged briefly to ensure that all reagents were thrown to the bottom of the reaction tube. The PCR reaction tube was put into ABI 7500 fluorescence quantitative PCR instrument for reaction. The amplification curve and dissolution curve were analyzed immediately after the reaction, and each sample was repeated three times. Reaction conditions were pre-denaturation at 95℃ for 10 min, denaturation at 95℃ for 10 s, annealing at 64℃ for 20 s, extension at 72℃ for 32 s, in a total of 40 cycles. This experiment was performed to calculate the relative expression of NRG-4, AKT1, mTOR, Cyclin D1, Bcl-2, Bax and caspase-3, with GADPH as the internal reference. Detection in cells was similar as that in tissues.

Western Blot for detecting NRG-4; ErbB2, ErbB4; MMP2, TGFβ1, α-SMA; Caspase3, Bax and Bcl-2 protein expressions

For the extraction of total protein of tissues, an appropriate amount of tissue was taken and put in a homogenizer, with the addition of 1 ml of pre-cooled PBS, homogenized until there was no obvious visible solid, transferred to a pre-cooled 1.5 ml EP tube, placed on ice for 5 min, and then the supernatant was transferred into another pre-cooled EP tube. The next step was centrifugation at 4℃ for 3min (500r/min), with the supernatant discarded. After that, every 20μL cells were added with 200μL pre-cooled buffer A and 2μL protease inhibitor mix to oscillate for 15s and then placed on ice for 10min. After repeated centrifugation at 4℃ for 5min (16,000r/min), the supernatant after centrifugation was transferred into a 0.5mL centrifuge tube and stored at - 80℃. After electrophoresis, the membrane was transferred directly by the wet transfer method, and then the transferred membrane was placed into a TBST sealing solution containing 5% skimmed milk powder for 1h of sealing at room temperature. For the incubation of the primary antibody, the sealed membrane was placed into the corresponding primary antibodies for overnight incubation at 4℃. For subsequent incubation of the secondary antibody, the treated membrane was washed with TBST buffer at 4℃ for 15min×3 times and added into the secondary antibody for 4h of incubation at 4℃. After washing with TBST buffer at 4℃ for 15min×3 times, the membrane was developed with ECL and exposed automatically in the chemiluminescence imaging system. The gray value of the target band was measured by Quantity One software, and the gray value of the experimental group and β-actin was calculated with β-actin as the control. The procedure of the cell experiment was similar to that of detection in tissues.

Methyl thiazolyl tetrazolium salt (MTT) colorimetry assay for cell activity detection

In the step of cell inoculation, rat cardiomyocytes were separated from suckling mice in the same steps as before, inoculated into 96 well plates at a cell concentration of $1 \times 10_3$-10_4 cells per well, and the volume of each well was 200μL. For cell culture, the cells were cultured in a carbon dioxide incubator (37℃, 5% CO_2) for 3-5 d. After 3-5 d of culture, 20 μl of MTT (5 mg/mL, prepared with PBS, pH = 7.4) was added to each well for continuous culture for 4 h. After that, the culture was terminated and the suspension in the well was sucked and discarded carefully. In the next step, 150μL DMSO was added to each well and oscillated for 10 min to make the crystal-melt completely. The wavelength of 490 nm was selected to measure the light absorption value of each well on the MTT enzyme-linked immunometric meter, and the results were recorded. The cell growth curve was drawn with time as abscissa and light absorption value as ordinate.

Flow cytometry for cell apoptosis detection

After 7 d of culture, the medium was removed, cells were washed with PBS once, digested with trypsin without EDTA for 30 s, and then digested with PBS containing 10% FBS. Trypsin digestion time should not be too long, otherwise, it was easy to cause false-positive results. Following centrifugation at 2,000 rpm for 5 min, cells were collected and washed with PBS once. With the adjustment of cell concentration at $1-5 \times 10^5$/mL, 500 μL Binding Buffer was a to mix well for incubation at room temperature for 5-15 min of reaction. The detection was performed by using a flow cytometer within 1 h. The four regions of the apoptotic graph were R1, normal cells; R2, early apoptotic cells; R3, late apoptotic cells; R4, necrotic cells. The apoptosis rate was calculated based on regions R2 and R3.

Statistical analysis

SPSS 21.0 software package (SPSS Inc, Chicago, IL, USA) was used to analyze the data and calculate the mean and standard deviation. All experiments were repeated at least three times. T-test was used for between-group data analysis. One-way analysis of variance was used for multiple-group analysis.

The presence of a significant difference was determined when $P<0.05$.

Results and discussion
**Myocardial staining results in SHR rats**

HE staining (Figure 1A) showed that the cardiomyocytes in the WKY group were smaller in size, more uniform in shape and arranged more orderly. In the SHR group, the cardiomyocytes were characterized by hypertrophy, disordered arrangement, hyperchromatic nucleus, irregular shape, obvious rupture of myocardial fibers, and obvious proliferation of fibrous stroma. According to Masson staining (Figure 1B), the myocardial fibers in the WKY group were arranged in order, there was a small amount of collagen deposition around the coronary artery in the myocardium, and the collagen in the myocardial interstitium was mostly long strip distribution. While in the SHR group, there was obvious myocardial fibrosis, and there were more blue collagen fibers around cardiomyocytes and myocardial arterioles; cardiomyocytes were swollen, muscle fibers arranged disorderly, collagen around the coronary artery and myocardial interstitium increased significantly with a cross-linking appearance. In addition, based on the results of Tunel staining, as shown in Figure 1C, compared with the WKY group, the apoptosis index of cardiomyocytes in the SHR group was significantly increased, with a statistical difference ($P<0.05$).

Expression of NRG-4 protein in myocardial tissue of SHR rats

As shown in Figure 2 of the results of the expression of NRG-4 detected by immunohistochemistry, NRG-4 protein was found to be expressed in the cytoplasm, and its positive expression was brown and granular in appearance. The semi-quantitative system was used to score the immunohistochemical staining, and the results were statistically analyzed, which showed that the expression of NRG-4 protein was significantly decreased in the SHR group, with statistical difference compared with the WKY group ($P<0.05$).
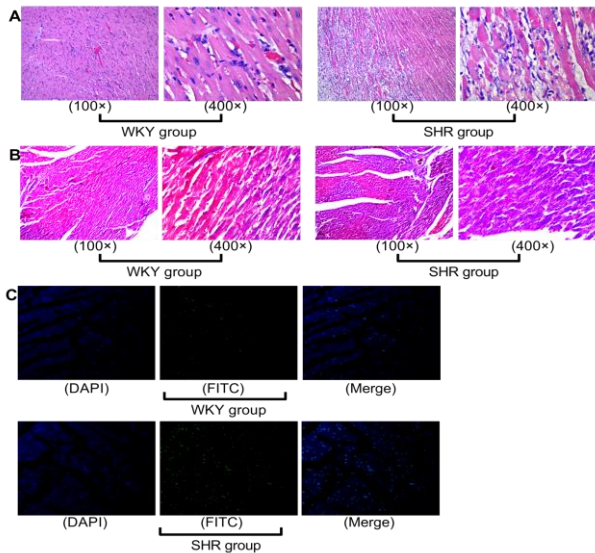
Figure 1. Myocardial staining results in SHR rats. Note: A: HE staining between WKY group and SHR group (100× and 400×); B: Masson staining between WKY group and SHR group (100× and 400×); C: Tunel staining between WKY group and SHR group.
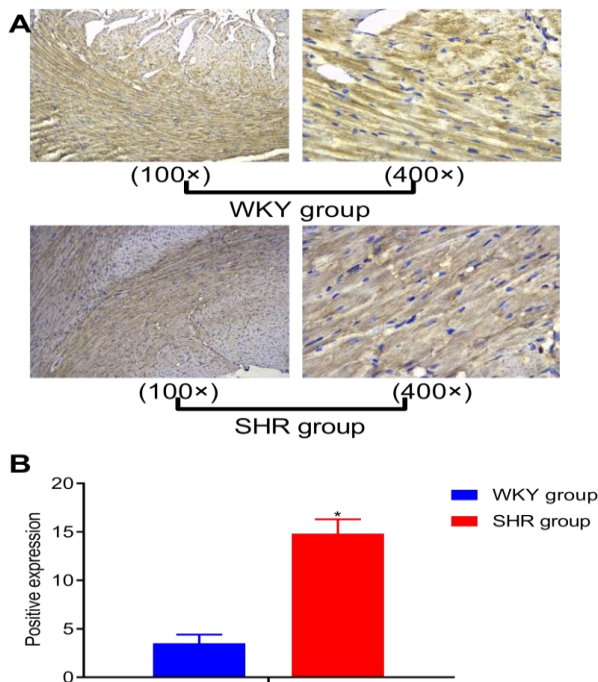
Figure 2. Expression of NRG-4 protein in myocardial tissue of SHR rats by immunohistochemistry. Note: A: Expression of NRG-4 protein in myocardial tissue by immunohistochemistry (100× and 400×); B: The semi-quantitative analysis of NRG-4 expression between WKY group and SHR group; *compared with WKY group, $P<0.05$.

Results of qRT-PCR and Western blot detection in each group

The relative mRNA expressions of NRG-4 and ErbB pathway-related genes (ErbB2 and ErbB4) were detected by qRT-PCR, and the results were analyzed by the $2^{-\Delta\Delta CT}$ method. The results (Figure 3A) showed that there was no obvious difference in the mRNA expression of NRG-4, ErbB2 and ErbB4 among the Control group, Empty vector group, shRNA NC group and pcDNA3.1(-) NC group (all $P>0.05$). While shRNA group showed significantly decreased mRNA expression of NRG-4, ErbB2 and ErbB4 when compared with shRNA NC group (all $P<0.05$); while compared with pcDNA3.1(-) NC group, pcDNA3.1(-) group had highly increased mRNA expression of NRG-4, ErbB2 and ErbB4 (all $P<0.05$).

Furthermore, a western blot was also performed to explore the protein expression of NRG-4, ErbB2 and ErbB4. Similarly, as shown in Figure 3BC, no obvious difference was found in the protein expression of the three proteins among the control group, empty vector group, shRNA NC group and pcDNA3.1(-) NC group (all $P>0.05$). In addition, the shRNA group had highly downregulated protein expression of NRG-4, ErbB2 and ErbB4 when compared with the shRNA NC group, which, however, was upregulated in pcDNA3.1(-) group relative to pcDNA3.1(-) NC group, with statistical differences (all $P<0.05$).

Results of MTT assay and expression levels of proliferation-related factors

MTT assay was used to detect the cell proliferation, and the results (Figure 4A) showed no obvious difference in cell proliferation among the control group, Empty vector group, shRNA NC group and pcDNA3.1(-) NC group (all $P>0.05$). While the rate of cell proliferation was downregulated in the shRNA group and upregulated in the pcDNA3.1(-) group when compared with the shRNA NC group and pcDNA3.1(-) NC group, respectively (all $P<0.05$).

As shown in Figure 4BCD in terms of the results of qRT-PCR and Western blot detection of fibrosis-related genes (MMP2, TGFβ1 and α-SMA), there was no obvious difference in their mRNA expression (all $P>0.05$). Furthermore, the shRNA group showed increased mRNA and protein expressions of MMP2, TGFβ1 and α-SMA when compared with the shRNA

NC group ($P<0.05$); while pcDNA3.1(-) group had decreased mRNA and protein expressions of MMP2, TGFβ1 and α-SMA, with statistical differences (all $P<0.05$).
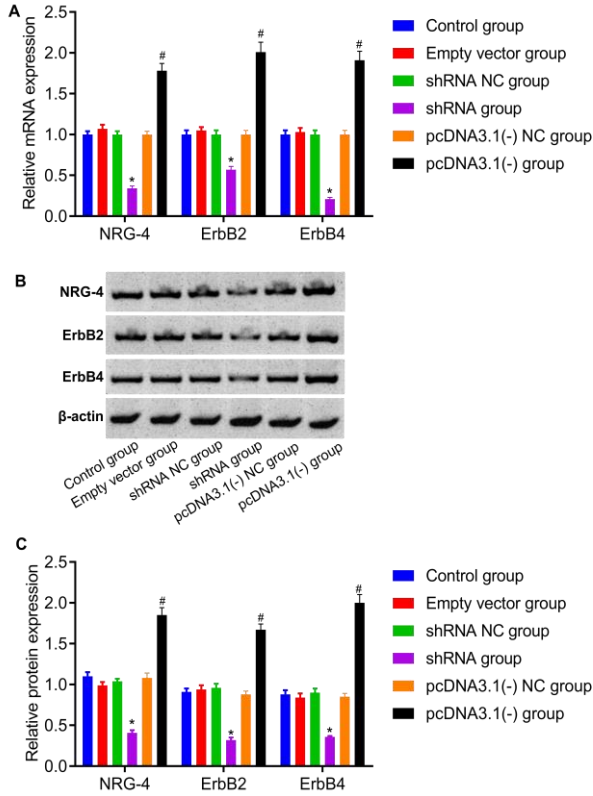
Figure 3. Results of qRT-PCR and Western blot detection of NRG-4 and ErbB pathway-related genes (ErbB2 and ErbB4) in each group. Note: A: Relative mRNA expression of NRG-4 gene and ErbB signaling pathway-related genes; B: Relative protein expression of NRG-4 gene and ErbB signaling pathway-related genes; C: Western blot images of NRG-4 and ErbB signaling pathway-related proteins; *, compared with shRNA NC group, $P<0.05$; #, compared with pcDNA3.1(-) NC group, $P<0.05$.

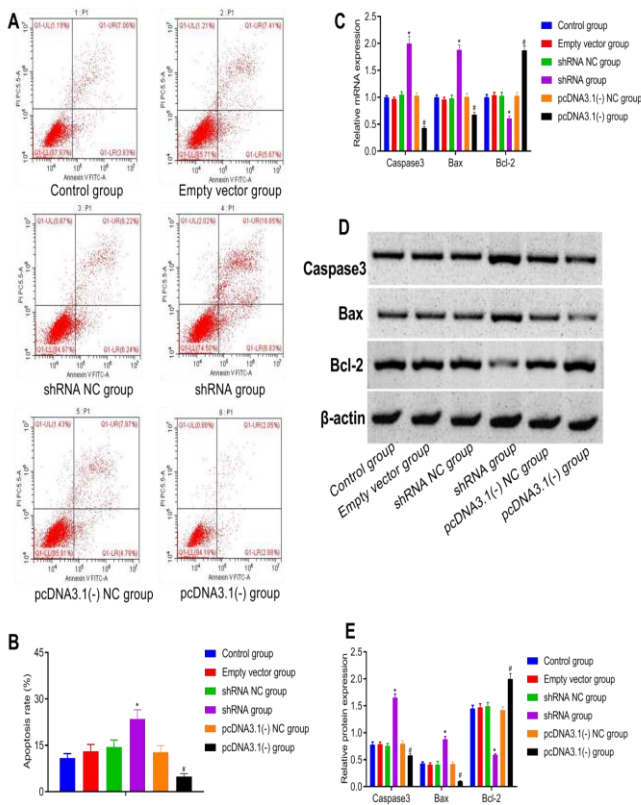**Results of flow cytometry and expression levels of apoptosis-related factors**

According to the detection results of cell apoptosis by using flow cytometry(Figure 5AB), there was no significant difference in cell apoptosis among the control group, empty vector group, shRNA NC group and pcDNA3.1(-) NC group (all $P>0.05$). However and significantly, the shRNA group showed increased cell apoptosis rate and the pcDNA3.1(-) group had decreased rate when compared with the shRNA NC group and pcDNA3.1(-) NC group, respectively (all $P<0.05$).
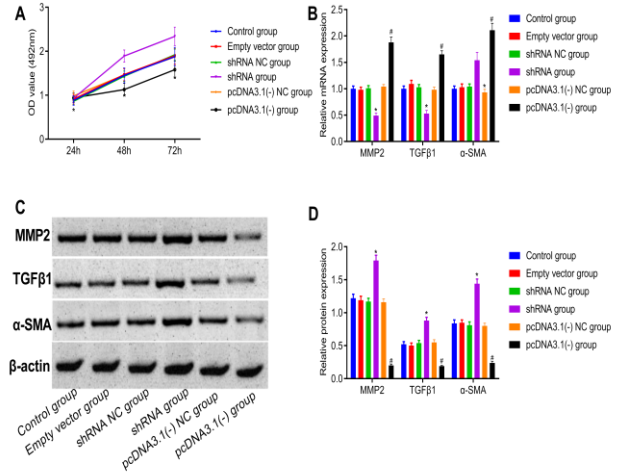
Figure 4. Results of MTT assay and expression levels of proliferation-related factors (MMP2, TGFβ1 and α-SMA) by qRT-PCR and Western blot in each group. Note: A: Results of MTT assay; B: Relative mRNA expression of MMP2, TGFβ1 and α-SMA; C: Relative protein expression of MMP2, TGFβ1 and α-SMA; D: Western blot images of MMP2, TGFβ1 and α-SMA; *, compared with shRNA NC group, $P<0.05$; #, compared with pcDNA3.1(-) NC group, $P<0.05$.

Furthermore, there was no significant difference in the mRNA and protein expression of apoptosis-related genes (Caspase3, Bax and Bcl-2) (all $P>0.05$). While in relative to the shRNA NC group, shRNA group showed increased mRNA and protein expression of Caspase3 and Bax, but decreased expression of Bcl-2 (all $P<0.05$). In addition, compared with pcDNA3.1(-) NC group, pcDNA3.1(-) group showed decreased mRNA and protein expression of Caspase3 and Bax, but increased expression of Bcl-2 (all $P<0.05$) (Figure 5CDE).

Nowadays, the incidence of hypertension is increasing year by year in China (30), and there are more than 200 million adult patients with hypertension in China (31). Hypertension is one of the main risk factors of cardiovascular and cerebrovascular diseases such as stroke and coronary heart disease (32). In China, hypertension has been confirmed to be the major risk factor for subjects who die from cardiovascular and cerebrovascular diseases (33). Target organ damage is the major death factor of hypertension (34). The treatment of hypertension is no longer just to reduce blood pressure to the normal range.

Figure 5. Results of flow cytometry and expression levels of apoptosis-related factors (Caspase3, Bax and Bcl-2) by qRT-PCR and Western blot in each group. Note: A: Results of flow cytometry; B: Statistical analysis of cell apoptosis; C: Relative mRNA expression of MMP2, TGFβ1 and α-SMA; D: Relative protein expression of MMP2, TGFβ1 and α-SMA; E: Western blot images of MMP2, TGFβ1 and α-SMA; *, compared with shRNA NC group, P<0.05; #, compared with pcDNA3.1(-) NC group, P<0.05.

It is critical to pay attention to the protection of target organs while controlling blood pressure (35). Significantly, patients with long-term hypertension may develop ventricular hypertrophy and myocardial fibrosis (14). Myocardial fibrosis is a complex pathological process (15). Myocardial fibrosis is a progressive, persistent and irreversible pathological change, which is the key pathological basis of heart failure (16). After myocardial infarction, interstitial fibrosis occurs not only in the infarcted area (17,18). At present, the drugs for the treatment of hypertensive myocardial fibrosis mainly include angiotensin-converting enzyme inhibitor (ACEI), angiotensin receptor inhibitor (ARB), aldosterone receptor inhibitor, P-receptor blocker, statins and natural drugs (36,37). While there is an increased concern about the side effects and limitations of chemicals, such as potassium retention in ACEI and ARB that should be

used cautiously for patients with renal insufficiency (38). It in turn highlights the importance of clarifying the molecular pathogenesis of the hypertensive myocardial fibrosis process and identifying possible targets for its treatment.

SHR is a kind of hypertension model which is very similar to the pathological performance of human essential hypertension (39). It belongs to polygenic hereditary hypertension and is quite similar to the pathogenesis and pathophysiological changes of human hypertension. It is an ideal animal model for the study of human essential hypertension and the screening of antihypertensive drugs (40). Lentiviral vector is a gene therapy vector based on the human immunodeficiency virus, which is a kind of retrovirus (41). In addition to the basic characteristics and structure of retrovirus, it also has a wider host range than retrovirus vector. Lentivirus has a higher titer than retrovirus. It can not only infect cells in the mitotic phase but also infect cells in the non-mitotic phase. It has the advantages of high transfection efficiency, low immunogenicity, no cellular immune response at the injection site, low humoral immune response and high safety (42). Lentiviral vectors can be used to study the regulation of promoters, overexpression of specific genes or silencing of specific genes, which are widely used in gene therapy. Specifically, the direct myocardial injection has good targeting and high transfection efficiency, but it needs thoracotomy under good anesthesia conditions to complete. Intracardiac or coronary injection often requires ligation of main and pulmonary arteries, and temporary cardiac arrest to achieve high transfection efficiency. These transfection methods are difficult to operate and have high mortality in rats. Hence in this experiment, the lentiviral vectors were injected into rats via tail vein. This method is simple, easy to operate, and more suitable for clinical application.

In our study, it was found that in rats with SHR, the cardiomyocytes showed hypertrophy, disordered arrangement, hyperchromatic nucleus, irregular shape, obvious rupture of myocardial fibers, and obvious proliferation of fibrous stroma; obvious myocardial fibrosis, and there were more blue collagen fibers around cardiomyocytes and myocardial arterioles; cardiomyocytes were swollen, muscle fibers arranged disorderly, collagen around the coronary artery and myocardial interstitium increased significantly with a

cross-linking appearance, as well as promoted apoptosis of, suggesting a pathological change in those modeling rats. Besides, the expression of NRG-4 protein was significantly decreased in SHR rats compared with WKY rats. To this end, we proposed our speculation that NRG-4 may be downregulated in SHR, and upregulation of NRG-4 may exert a potential positive role in alleviating the progression of SHR. Accordingly, there was no obvious difference in the mRNA expression of NRG-4, ErbB2 and ErbB4, MMP2, TGFβ1 and α-SMA, as well as Caspase3, Bax and Bcl-2 among the control group, Empty vector group, shRNA NC group and pcDNA3.1(-) NC group. While significantly, after downregulation of the expression of NRG-4, the expressions of NRG-4 were silenced, supporting a successful downregulation treatment of this gene. Meanwhile, ErbB2 and ErbB4 were both downregulated, which may reveal a possible inactivation of the ErbB signaling pathway. While upregulation of NRG-4 resulted in increased NRG-4 expression and activated ErbB2 and ErbB4. In general, NRG is an epidermal growth factor-like protein, which is a member of the Neuregulin family (23). It can activate downstream signaling pathways by binding with the tyrosine kinase receptors ErbB3 and ErbB4 on the cell surface (25). NRG plays an important role in tissue development, survival of epidermal cells, cell growth and differentiation (20). Meanwhile, as a growth factor, the expression level of NRG in the human body is closely related to breast cancer (43), gallbladder cancer, renal cell carcinoma, bladder cancer, ovarian cancer, pancreatic cancer (44), and hypertension (45). Recently, NRG is defined as an endocrine factor in brown adipose tissue (46), which can improve diet-induced insulin resistance and hepatic steatosis by inhibiting liver lipid synthesis and chronic inflammatory response, promoting liver fatty acid oxidation and energy consumption, which may facilitate the attenuating of sympathetic activity and blood pressure.

Furthermore, downregulated NRG-4 expression resulted in promoted cardiomyocyte proliferation and apoptosis, while upregulated expression was associated with inhibited cardiomyocyte proliferation and apoptosis. As for the exploration of mechanism, downregulation of NRG-4 resulted in increased MMP2, TGFβ1, α-SMA and Bcl-2, while increased Caspase3 and Bax expressions; while its upregulation decreased MMP2, TGFβ1, α-SMA and Bcl-2, while reduced Caspase3 and Bax expressions. For the interpretation and explanation of the above results, MMP-2 is a gelatin matrix metalloproteinase, which can release the angiogenesis-related factors stored in ECM by degrading ECM and promoting the formation of blood vessels (47). Recent studies have found that MMP-2 can promote angiogenesis by stimulating the expression of VEGF; MMP-2 is expressed in a variety of cells, including endothelial cells and cardiac fibroblasts; MMP-2 plays an important role in the cardiovascular system, and can inhibit the contractile function of the myocardium (48,49). In addition, TGF-β1 is an important member of the TGF-β multi-functional family (50). It is a powerful promoter of synthesis and deposition of collagen fibers and other extracellular factors and is closely related to fibrosis of many organs (50). Prior research has confirmed that the expression of TGF-β1 increased significantly in the myocardial tissue of the myocardial infarction rat model (51). While as a kind of myocardial interstitial cells, α-SMA is high in quantity and is closest to myocardial cells (52). It can inhibit extracellular matrix-degrading enzymes, promote myocardial fibrosis and play an important role in the development of myocardial fibrosis (52). In vitro experiments also showed that TGF-β1 could promote the proliferation and transformation of cardiac fibroblasts into myofibroblasts, promote the expression of α-SMA in fibroblasts, and produce a large amount of extracellular matrices, such as collagen fibers and fibronectin (53). In our in vitro test, downregulation of MMP2, TGFβ1, α-SMA resulted from upregulation of NRG-4 did support the anti-proliferation and anti-fibrosis progression of cardiomyocytes. Meanwhile, it is well known that Bcl-2 is an important anti-apoptotic factor while Caspase3 and Bax are pro-apoptotic factors (54). The reduced Caspase3 and Bax expressions but increased Bcl-2 expression supported the anti-apoptosis role exerted by downregulated NRG-4 expression.

With regard to the aforementioned findings, it inspires us that the use of recombinant NRG-4 to intervene the cardiac signal transduction and improve cardiac function has a strong potential therapeutic value. However, the clear mechanism of the cardiovascular effect of this signaling pathway still needs to be further studied; besides, the use of small

molecule ErbB receptor agonists may also be a potential direction in our future study. In addition, this study confirmed that NRG-4 can participate in the proliferation and apoptosis of cardiomyocytes, and mediate the process of myocardial fibrosis. However, it is not clear whether NRG is involved clearly in improving cardiac function. Anyway, the current research in this field is still preliminary, and a clear understanding of the above mechanism is the premise for NRG to be formally applied in clinical practice, which is the major highlight of this study.

In conclusion, our study confirms that upregulation of NRG-4 gene expression can promote the activation of the ErbB signaling pathway, thus inhibiting the proliferation and apoptosis of cardiomyocytes in SHR rats, reversing myocardial fibrosis, and playing its cardioprotective role. In our subsequent research, we should further explore the related molecular mechanism, detect more related transcription factors and signaling molecules, and find the downstream molecular mechanism of NRG-4 regulating the expression of related factors, so as to improve the understanding of NRG-4 regulating fibrosis mechanism.

Acknowledgments

Conflict interest

The authors declare no conflict of interest.

References

1. Ma J, Li H. The Role of Gut Microbiota in Atherosclerosis and Hypertension. Front Pharmacol. 2018;9:1082.

2. Fatkhullina AR, Peshkova IO, Koltsova EK. The Role of Cytokines in the Development of Atherosclerosis. Biochemistry (Mosc). 2016;81(11):1358-1370.

3. Xu L, Brink M. mTOR, cardiomyocytes and inflammation in cardiac hypertrophy. Biochim Biophys Acta. 2016;1863(7 Pt B):1894-903.

4. van Rooij E, Sutherland LB, Liu N, Williams AH, McAnally J, Gerard RD, Richardson JA, Olson EN. A signature pattern of stress-responsive microRNAs that can evoke cardiac hypertrophy and heart failure. Proc Natl Acad Sci U S A. 2006 Nov 28;103(48):18255-60.

5. Nomura S, Satoh M, Fujita T, Higo T, Sumida T, Ko T, Yamaguchi T, Tobita T, Naito AT, Ito M, Fujita K, Harada M, Toko H, Kobayashi Y, Ito K, Takimoto E, Akazawa H, Morita H, Aburatani H, Komuro I. Cardiomyocyte gene programs encoding morphological and functional signatures in cardiac hypertrophy and failure. Nat Commun. 2018;9(1):4435.

6. Meissner A. Hypertension and the Brain: A Risk Factor for More Than Heart Disease. Cerebrovasc Dis. 2016;42(3-4):255-62.

7. Pillai A, Sharma D, Kadam P. Hypertension in the Neonatal Period: An Update. Curr Hypertens Rev. 2016;12(3):186-195.

8. Rostami Ahmadvandi, H., Faghihi, A. Adapted Oilseed Crops with the Ability to Grow Economically in Dryland Conditions in Iran. Agrotech Ind Crops, 2021; 1(3): 122-128. doi: 10.22126/atic.2021.6518.1015

9. Du J, Zhang C, Zhao W. Autophagy and Hypertension. Adv Exp Med Biol. 2020;1207:213-216.

10. Konukoglu D, Uzun H. Endothelial Dysfunction and Hypertension. Adv Exp Med Biol. 2017;956:511-540.

11. Sitia S, Tomasoni L, Atzeni F, Ambrosio G, Cordiano C, Catapano A, Tramontana S, Perticone F, Naccarato P, Camici P, Picano E, Cortigiani L, Bevilacqua M, Milazzo L, Cusi D, Barlassina C, Sarzi-Puttini P, Turiel M. From endothelial dysfunction to atherosclerosis. Autoimmun Rev. 2010;9(12):830-4.

12. Kostov K, Halacheva L. Role of Magnesium Deficiency in Promoting Atherosclerosis, Endothelial Dysfunction, and Arterial Stiffening as Risk Factors for Hypertension. Int J Mol Sci. 2018;19(6):1724.

13. de Boer RA, De Keulenaer G, Bauersachs J, Brutsaert D, Cleland JG, Diez J, Du XJ, Ford P, Heinzel FR, Lipson KE, McDonagh T, Lopez-Andres N, Lunde IG, Lyon AR, Pollesello P, Prasad SK, Tocchetti CG, Mayr M, Sluijter JPG, Thum T, Tschöpe C, Zannad F, Zimmermann WH, Ruschitzka F, Filippatos G, Lindsey ML, Maack C, Heymans S. Towards better definition, quantification and treatment of fibrosis in heart failure. A scientific roadmap by the Committee of Translational Research of the Heart Failure Association (HFA) of the European Society of Cardiology. Eur J Heart Fail. 2019;21(3):272-285.

14. Nadruz W. Myocardial remodeling in hypertension. J Hum Hypertens. 2015;29(1):1-6.

15. Frump AL, Bonnet S, de Jesus Perez VA, Lahm T. Emerging role of angiogenesis in adaptive and maladaptive right ventricular remodeling in pulmonary hypertension. Am J Physiol Lung Cell Mol Physiol. 2018 Mar;314(3):L443-L460.

16. Hinz B, Lagares D. Evasion of apoptosis by myofibroblasts: a hallmark of fibrotic diseases. Nat Rev Rheumatol. 2020;16(1):11-31.

17. Gyöngyösi M, Winkler J, Ramos I, Do QT, Firat H, McDonald K, González A, Thum T, Díez J, Jaisser F, Pizard A, Zannad F. Myocardial fibrosis: biomedical research from bench to bedside. Eur J Heart Fail. 2017;19(2):177-191.

18. Espeland T, Lunde IG, H Amundsen B, Gullestad L, Aakhus S. Myocardial fibrosis. Tidsskr Nor Laegeforen. 2018;138(16).

19. González A, López B, Ravassa S, San José G, Díez J.

The complex dynamics of myocardial interstitial fibrosis in heart failure. Focus on collagen cross-linking. Biochim Biophys Acta Mol Cell Res. 2019;1866(9):1421-1432.

20. Lai D, Liu X, Forrai A, Wolstein O, Michalicek J, Ahmed I, Garratt AN, Birchmeier C, Zhou M, Hartley L, Robb L, Feneley MP, Fatkin D, Harvey RP. Neuregulin 1 sustains the gene regulatory network in both trabecular and nontrabecular myocardium. Circ Res. 2010;107(6):715-27.

21. Ieguchi K, Fujita M, Ma Z, Davari P, Taniguchi Y, Sekiguchi K, Wang B, Takada YK, Takada Y. Direct binding of the EGF-like domain of neuregulin-1 to integrins ({alpha}v{beta}3 and {alpha}6{beta}4) is involved in neuregulin-1/ErbB signaling. J Biol Chem. 2010 Oct 8;285(41):31388-98.

22. Kogata N, Zvelebil M, Howard BA. Neuregulin 3 and erbb signalling networks in embryonic mammary gland development. J Mammary Gland Biol Neoplasia. 2013;18(2):149-54.

24. Brown N, Deb K, Paria BC, Das SK, Reese J. Embryo-uterine interactions via the neuregulin family of growth factors during implantation in the mouse. Biol Reprod. 2004;71(6):2003-11.

25. Sun Y, Yang Z, Zheng B, Zhang XH, Zhang ML, Zhao XS, Zhao HY, Suzuki T, Wen JK. A Novel Regulatory Mechanism of Smooth Muscle α-Actin Expression by NRG-1/circACTA2/miR-548f-5p Axis. Circ Res. 2017;121(6):628-635.

26. Takahashi Y, Uchino A, Shioya A, Sano T, Matsumoto C, Numata-Uematsu Y, Nagano S, Araki T, Murayama S, Saito Y. Altered immunoreactivity of ErbB4, a causative gene product for ALS19, in the spinal cord of patients with sporadic ALS. Neuropathology. 2019;39(4):268-278.

27. Di Segni A, Farin K, Pinkas-Kramarski R. ErbB4 activation inhibits MPP+-induced cell death in PC12-ErbB4 cells: involvement of PI3K and Erk signaling. J Mol Neurosci. 2006;29(3):257-67.

28. Deng W, Luo F, Li BM, Mei L. NRG1-ErbB4 signaling promotes functional recovery in a murine model of traumatic brain injury via regulation of GABA release. Exp Brain Res. 2019;237(12):3351-3362.

29. Dugaucquier L, Feyen E, Mateiu L, Bruyns TAM, De Keulenaer GW, Segers VFM. The role of endothelial autocrine NRG1/ERBB4 signaling in cardiac remodeling. Am J Physiol Heart Circ Physiol. 2020;319(2):H443-H455.

30. Wang Z, Chen Z, Zhang L, Wang X, Hao G, Zhang Z, Shao L, Tian Y, Dong Y, Zheng C, Wang J, Zhu M, Weintraub WS, Gao R; China Hypertension Survey Investigators. Status of Hypertension in China: Results From the China Hypertension Survey, 2012-2015. Circulation. 2018;137(22):2344-2356.

31. Su M, Zhang Q, Bai X, et al. Availability, cost, and prescription patterns of antihypertensive medications in primary health care in China: a nationwide cross-

sectional survey. Lancet. 2017 Dec 9;390(10112):2559-2568.

32. Fe A, Rel B, Pm A, et al. Knowledge On Arterial Hypertension In General Population: Results From A Community Pharmacy Screening Program. Nutrition, Metabolism and Cardiovascular Diseases, 2021.

33. Ma J, Li H. The Role of Gut Microbiota in Atherosclerosis and Hypertension. Front Pharmacol. 2018 Sep 25;9:1082.

34. Cai W, Lang MJ, Jiang XB, et al. Correlation among high salt intake, blood pressure variability, and target organ damage in patients with essential hypertension: Study protocol clinical trial (SPIRIT compliant). Medicine, 2020, 99(14):e19548.

35. Luca M, Sorriento D, Massa D, et al. Effects of inhibition of the renin-angiotensin system on hypertension-induced target organ damage: Clinical and experimental evidence. 2021; 91(1).

36. Spannella F, Giulietti F, Balietti P, et al. Renin-Angiotensin System Blockers and Statins Are Associated With Lower In-Hospital Mortality in Very Elderly Hypertensives. J Am Med Dir Assoc. 2018;19(4):342-347.

37. Prasad K, Mishra M. Do Advanced Glycation End Products and Its Receptor Play a Role in Pathophysiology of Hypertension? Int J Angiol. 2017;26(1):1-11.

38. Villa-Zapata L, Carhart BS, Horn JR, et al. Serum potassium changes due to concomitant ACEI/ARB and spironolactone therapy: A systematic review and meta-analysis. Am J Health Syst Pharm. 2021;78(24):2245-2255.

39. Vendruscolo LF, Izídio GS, Takahashi RN. Drug reinforcement in a rat model of attention deficit/hyperactivity disorder--the Spontaneously Hypertensive Rat (SHR). Curr Drug Abuse Rev. 2009;2(2):177-83.

40. Meneses A, Perez-Garcia G, Ponce-Lopez T, Tellez R, Gallegos-Cari A, Castillo C. Spontaneously hypertensive rat (SHR) as an animal model for ADHD: a short overview. Rev Neurosci. 2011;22(3):365-71.

41. Milone MC, O'Doherty U. Clinical use of lentiviral vectors. Leukemia. 2018 Jul;32(7):1529-1541.

42. Escors D, Breckpot K. Lentiviral vectors in gene therapy: their current status and future potential. Arch Immunol Ther Exp (Warsz). 2010;58(2):107-19.

43. De Iuliis F, Salerno G, Taglieri L, Lanza R, Cardelli P, Scarpa S. Circulating neuregulin-1 and galectin-3 can be prognostic markers in breast cancer. Int J Biol Markers. 2017;32(3):e333-e336.

44. Jonna S, Feldman RA, Swensen J, Gatalica Z, Korn WM, Borghaei H, Ma PC, Nieva JJ, Spira AI, Vanderwalde AM, Wozniak AJ, Kim ES, Liu SV. Detection of NRG1 Gene Fusions in Solid Tumors. Clin Cancer Res. 2019;25(16):4966-4972.

45. Matsukawa R, Hirooka Y, Ito K, Sunagawa K. Inhibition of neuregulin-1/ErbB signaling in the rostral

ventrolateral medulla leads to hypertension through reduced nitric oxide synthesis. Am J Hypertens. 2013;26(1):51-7.

46. Guo L, Zhang P, Chen Z, Xia H, Li S, Zhang Y, Kobberup S, Zou W, Lin JD. Hepatic neuregulin 4 signaling defines an endocrine checkpoint for steatosis-to-NASH progression. J Clin Invest. 2017 Dec 1;127(12):4449-4461.

47. Boelen GJ, Boute L, d'Hoop J, EzEldeen M, Lambrichts I, Opdenakker G. Matrix metalloproteinases and inhibitors in dentistry. Clin Oral Investig. 2019;23(7):2823-2835.

48. Huang ST, Chang CC, Pang JS, Huang HS, Chou SC, Kao MC, You HL. Drynaria fortunei Promoted Angiogenesis Associated With Modified MMP-2/TIMP-2 Balance and Activation of VEGF Ligand/Receptors Expression. Front Pharmacol. 2018;9:979.

49. Hardy E, Hardy-Sosa A, Fernandez-Patron C. MMP-2: is too low as bad as too high in the cardiovascular system? Am J Physiol Heart Circ Physiol. 2018;315(5):H1332-H1340.

50. Ji W, Wang X, Zhao C. [Expression of TGF-beta1 and collagen fibers in chronic nasal-sinusitis nasal mucosa of patients]. Lin Chung Er Bi Yan Hou Tou Jing Wai Ke Za Zhi. 2014;28(11):756-9. Chinese.

51. Han A, Lu Y, Zheng Q, Zhang J, Zhao Y, Zhao M, Cui X. Qiliqiangxin Attenuates Cardiac Remodeling via Inhibition of TGF-β1/Smad3 and NF-κB Signaling Pathways in a Rat Model of Myocardial Infarction. Cell Physiol Biochem. 2018;45(5):1797-1806.

52. Wu X, Li M, Chen SQ, Li S, Guo F. Pin1 facilitates isoproterenol-induced cardiac fibrosis and collagen deposition by promoting oxidative stress and activating the MEK1/2-ERK1/2 signal transduction pathway in rats. Int J Mol Med. 2018;41(3):1573-1583.

53. Guo Y, Dong Z, Shi Y, Wang W, Wang L, Sun J, Sun X, Tian Z, Yao J, Li Z, Cheng J, Tian Y. Sonodynamic Therapy Inhibits Fibrogenesis in Rat Cardiac Fibroblasts Induced by TGF-β1. Cell Physiol Biochem. 2016;40(3-4):579-588.

54. Zhao T, Fu Y, Sun H, Liu X. Ligustrazine suppresses neuron apoptosis via the Bax/Bcl-2 and caspase-3 pathway in PC12 cells and in rats with vascular dementia. IUBMB Life. 2018;70(1):60-70.